Molecular Basis of Passive Stress Relaxation in Human Soleus Fibers: Assessment of the Role of Immunoglobulin-Like Domain Unfolding

K. Trombitás,* Y. Wu,* M. McNabb,* M. Greaser,† M. S. Z. Kellermayer,‡ S. Labeit,§ and H. Granzier*

*Veterinary and Comparative Anatomy, Pharmacology and Phisiology, Washington State University, Pullman, Washington 99164-6520 USA; †Muscle Biology Laboratory, University of Wisconsin 53706 Madison, Wisconsin USA; ‡Biophysics, University of Pécs Medical School, Pécs H-7624, Hungary; and §Anesthesiology and Intensive Operative Medicine, University Hospital Mannheim, 68135 Mannheim, Germany

ABSTRACT Titin (also known as connectin) is the main determinant of physiological levels of passive muscle force. This force is generated by the extensible I-band region of the molecule, which is constructed of the PEVK domain and tandem-immunoglobulin segments comprising serially linked immunoglobulin (Ig)-like domains. It is unresolved whether under physiological conditions Ig domains remain folded and act as "spacers" that set the sarcomere length at which the PEVK extends or whether they contribute to titin's extensibility by unfolding. Here we focused on whether Ig unfolding plays a prominent role in stress relaxation (decay of force at constant length after stretch) using mechanical and immunolabeling studies on relaxed human soleus muscle fibers and Monte Carlo simulations. Simulation experiments using Ig-domain unfolding parameters obtained in earlier single-molecule atomic force microscopy experiments recover the phenomenology of stress relaxation and predict large-scale unfolding in titin during an extended period ($>\sim$20 min) of relaxation. By contrast, immunolabeling experiments failed to demonstrate large-scale unfolding. Thus, under physiological conditions in relaxed human soleus fibers, Ig domains are more stable than predicted by atomic force microscopy experiments. Ig-domain unfolding did not become more pronounced after gelsolin treatment, suggesting that the thin filament is unlikely to significantly contribute to the mechanical stability of the domains. We conclude that in human soleus fibers, Ig unfolding cannot solely explain stress relaxation.

INTRODUCTION

When nonactivated striated muscle is stretched, passive force ensues. Passive force is derived from the intracellular titin filaments and intermediate filaments (IFs), and the extracellular protein collagen (Wang et al., 1993). Within the physiological sarcomere length range (in skeletal muscle $\sim$2.0–4.0 μm), titin is the main source of passive force, with IFs and collagen contributing mainly toward the upper end of the physiological length range and beyond it. Passive force prevents the overstretch of muscle, restores muscle length after release, and prevents sarcomere-length inhomogeneity and A-band translocation (away from its central position within the sarcomere), all of which are critical for efficient muscle contraction (Granzier et al., 1991; Horowits and Podolsky, 1987). Evidence obtained earlier in insect flight muscle (Granzier and Wang, 1993b), and more recently in cardiac muscle (Cazorla et al., 1999, 2001; Fukuda et al., 2001), suggests that passive force may also enhance actomyosin interaction, possibly via an effect of passive force on interfilament lattice spacing and/or thick filament structure (Cazorla et al., 2001; Fukuda et al., 2001). Thus, study of the molecular mechanisms that underlie passive force development and its adjustments (such as stress relaxation) is required for understanding both passive and active muscle function.

Titin, the main determinant of physiological levels of passive muscle force, is a filamentous protein that spans the half sarcomere (for recent reviews, see Granzier and Labeit, 2002; Gregorio et al., 1999; Horowits, 1999; Linke, 2000; Tskhovrebova and Trinick, 2002). Titin is anchored to the Z-line and M-line regions of the sarcomere and is attached to the thick filaments of the A-band. Passive force is generated by extension of the I-band region of titin, which is a serially connected chain of proximal (near the Z-line) and distal (near the A-band) tandem-Ig segments (tandem array of Ig-like domains) separated by the proline (P), glutamate (E)-, valine (V)-, and lysine (K)-rich PEVK sequence (Labeit and Kolmerer, 1995; Linke et al., 1996). When slack sarcomeres (lengths $\sim$2.0 μm) are stretched, initially the extension of tandem-Ig segments dominates, followed by PEVK extension at nearly constant tandem-Ig segment length (Linke et al., 1998b; Trombitas et al., 1998b). This constant length can be accommodated by Ig domains that maintain their native conformation (a seven-stranded β-barrel) (Improta et al., 1996), suggesting that lengthening of tandem-Ig segments in short sarcomeres results from segment straightening (due to unbending of sequences that link the Ig domains), whereas individual domains do not unfold (Trombitas et al., 1998a,b). Initially it was thought that this mechanism applied only to skeletal muscle. Cardiac muscle expresses short length variants of titin, with tandem-Ig and PEVK segments that are too short to accommodate titin's necessary length change in the physiological sarcomere length range, unless Ig domain unfolding takes place (Granzier et al., 1997). However, the subsequent discovery of an additional source of extensibility in cardiac titins (Helmes et al., 1999; Linke et al., 1999; Trombitas et al., 1999) alleviated the need for unfolding and resulted in the notion that under physiological

Submitted May 12, 2003, and accepted for publication July 25, 2003.

Address reprint requests to Henk L. Granzier, PhD, Dept. VCAPP, Washington State University, Pullman, WA 99164-6520. Tel.: 509-335-3390; Fax: 509-335-4650; E-mail: granzier@wsunix.wsu.edu.

0006-3495/03/11/3142/12 $2.00

conditions, in skeletal as well as cardiac muscles, Ig domains are stable and do not unfold (Linke and Granzier, 1998). Definitive evidence, however, has not been obtained.

The mechanical properties of titin have been explored in single-molecule manipulation experiments, revealing that the molecule behaves as a wormlike-chain entropic spring in which unfolding of the globular domains occurs at high force during stretch (Kellermayer et al., 1997; Rief et al., 1997; Tskhovrebova et al., 1997) and refolding at low force during release (Kellermayer et al., 1997). Subsequent studies (Carrion-Vazquez et al., 2000, 1999; Watanabe et al., 2002a) focused on characterizing the unfolding of Ig domains, using engineered protein fragments and atomic force microscopy (AFM). It was shown that if tandem-Ig segments are stretched, Ig domains unfold with a probability that increases with increasing force and passing time. A recent study (Minajeva et al., 2001) conducted a simulation of Ig domain unfolding, using kinetic parameters obtained from single-molecule AFM experiments, and predicted that unfolding of a few Ig domains may take place in myofibrils that are stretched and then held for 4 s at a fixed length. Our goal was to experimentally test for Ig domain unfolding by stretching and holding relaxed muscle for extended durations. Human soleus muscle was selected for this work because it is the only skeletal muscle type that expresses a titin isoform that has been completely sequenced (Labeit and Kolmerer, 1995). We studied stress relaxation in relaxed human soleus fibers and used immunoelectron microscopy (IEM), mechanics, and Monte Carlo simulations that take into account unfolding/refolding kinetics of Ig domains. Simulations confirm that AFM-based unfolding characteristics predict the unfolding of a few (~4) domains during short-term (~10 s) hold protocols, and that this can account for the measured stress relaxation. The same unfolding characteristics predict that, when the hold period is extended to 20 min or more, large-scale unfolding takes place (~70 domains in 1 h) and that, as a result, tandem-Ig segments should greatly lengthen (at the expense of the PEVK segment). However, the results of our IEM studies are inconsistent with this prediction and failed to reveal evidence for large-scale Ig unfolding. We conclude that in relaxed human soleus fibers, Ig unfolding is an unlikely event that cannot solely explain physiological levels of stress relaxation. We propose an alternative model with a prominent role for the PEVK region of titin.

MATERIALS AND METHODS

Mechanics

Single muscle fibers dissected from human soleus muscle (biopsies obtained in accordance with protocol ''Role of Titin in Human Muscle Tissue 2,'' Washington State University) were mechanically and chemically skinned. The fibers were kept in relaxing solution containing high concentrations of protease inhibitors and were used within 48 h of harvest (for technical details and solution composition, see Granzier et al., 1996; Granzier and Irving, 1995). Passive tension was measured with a strain gauge force transducer, and fiber length was controlled by a high-speed motor. Preparations were attached to the motor arm and the force transducer via aluminum clips. The width and the height of the fiber were measured and the cross-sectional area (CSA) was calculated assuming the cross section is elliptical in shape (Wu et al., 2000). The area (5400 ± 800 μm^2) was used to convert the measured force per fiber to tension (force/cross-sectional area). To obtain the passive tension versus sarcomere length (SL) relation, relaxed fibers (lengths 1.55 ± 0.15 mm) were slowly stretched (100 nm/s/half-sarcomere) from their slack SL (~2.0 μm) to predetermined amplitude, followed by hold of various durations (10 s to 60 min) and a release back to the slack length. SL was measured online by using laser diffraction (Granzier and Irving, 1995). The first-order diffraction line was projected onto a photodiode array, and the array was scanned 1000 times per second. Both the peak position and the width of the diffraction peak at the half-maximal height did not change during the long hold periods, suggesting that there were no significant redistributions of sarcomere lengths during this time. After a 20-min rest at slack, the protocol was repeated. Provided this rest period was included and the maximal SL amplitude was less than ~4.25 μm, results were highly reproducible. Experiments were performed at 20° to 22°C.

In addition to titin, intermediate filaments (IFs) also develop tension in passive muscle fibers, especially at long SLs (Granzier and Wang, 1993c; Wang et al., 1993). (Note that fibers had been mechanically skinned (as well as chemically skinned), which eliminates collagen as a source of passive tension.) To determine the force produced by IFs, skinned muscle fibers were incubated for 30 min with relaxing solution containing 0.6 M KCl followed by a 30-min incubation in relaxing solution containing 1.0 M KI. These solutions extract thick and thin filaments from the sarcomere, respectively, resulting in a loss of titin anchorage and hence titin-dependent passive force (Granzier and Wang, 1993c; Wang et al, 1993). Considering the extraction-resistant nature of IFs (Price, 1984), the remaining passive force after KCl/KI extraction (''KCl/KI-insensitive force'') may be assumed to derive from IFs, and the KCl/KI-sensitive force from titin (Granzier and Wang, 1993c; Wang et al,. 1993). Measured titin-based tension (in mN/mm^2) was converted to force per titin molecule assuming 1), that 80% of the cross-sectional fiber area is myofibril; 2), 470 thick filaments per μm^2 myofibril (based on the myofilament lattice spacing measured by x-ray diffraction on skinned muscle fibers at their slack length); and 3), six titin molecules per half thick filament. (For details and original citations see Cazorla et al., 2000; Granzier and Irving, 1995; Liversage et al., 2001). The same conversion factors were used in Fig. 3 *A* to extrapolate simulated single-titin force (in pN) to titin-based passive tension of single fibers (in mN/mm^2).

Immunoelectron microscopy

IEM methods have been published earlier (Granzier et al., 1996; Trombitas et al., 1991, 1998a, 1998b). Briefly, skinned fibers were stretched, held at fixed length (protocol as explained above; temperature ~4°C), then, after a predetermined hold period, they were fixed for 45 min by replacing the relaxing solution with freshly prepared 3% paraformaldehyde in phosphate-buffered saline (PBS). Fibers were then washed, blocked with bovine serum albumin (BSA), washed, and incubated for ~24 h with anti-titin antibodies in PBS/BSA. The following antibodies were used (see also Fig. 4 *A*): anti-I2/I3 (T12), anti-I80/I81 (N2A), anti-C-terminal PEVK residues (4596–4606 of human cardiac titin) (514), anti-I84/I85/I86 (formerly known as I20/I21/I22), anti-I109/I110/I11 (MIR epitope), anti-I111/I112 (Ti-102). For additional information on T12, see Furst et al., 1988, and Sebestyen et al., 1995; on 514, see Trombitas et al., 1998a; on Ti-102, see Jin, 1995, and Trombitas et al., 1998a; and for all other antibodies, see Bang et al., 2001. Fibers were then washed, labeled with secondary antibody, washed, fixed with glutaraldehyde/tannic acid, osmicated, and embedded in araldite. (Further details can be found in our publications cited above.) Ultrathin sections were stained with potassium permanganate and lead citrate and observed with a JEOL 1200 electron microscope. Mid-Z-line to mid-epitope distances were measured from electron micrographs following high-

resolution scanning and digital image processing using custom-written macros for the image analysis program NIH Image (v. 1.61,Wayne Rasband, National Institutes of Health). For spatial calibration, the electron microscope's magnification was used.

Thin filament extraction

The gelsolin clone FX-45 (Yu et al., 1991) containing the N-terminal half of human gelsolin constructed in a pET3D expression vector was used. Expression and purification were as described (Trombitas and Granzier, 1997). Fibers were incubated in gelsolin (~0.4 mg/ml) in relaxing solution for ~24 h, with continuous vigorous shaking (Granzier and Wang, 1993c). Actin extraction was verified by 1), activating the fibers, and 2), solubilizing the fibers and performing gel electrophoresis. Gel electrophoresis was performed as explained earlier (Cazorla et al., 2000); gels were silver-stained (Granzier and Wang, 1993a).

Analysis of force data

Force (F) data were compared with the wormlike chain (WLC) Eq. 1:

$$\frac{FP}{k_BT} = \frac{z}{C} + \frac{1}{4(1 - z/C)^2} - \frac{1}{4} \quad (1)$$

(Bustamante et al., 1994). The WLC model describes the molecule as a deformable continuum of persistence length P (measure of bending rigidity) and contour length C. The end-to-end length of the molecule is z and the fractional extension is z/C. The elastic region of titin in the sarcomere was modeled as three serially linked WLCs with different contour and persistence lengths: 1), native tandem-Ig segment, 2), unfolded tandem-Ig segment, and 3), PEVK segment. The contour length of the native tandem-Ig segments was calculated (Trombitas et al., 1998b) from the combined number of folded Ig domains times the maximal domain spacing (5 nm). The persistence length of the native tandem-Ig segment was set as 15 nm, based on several earlier studies (Higuchi et al., 1993; Tskhovrebova and Trinick, 2001). The contour length of the PEVK and unfolded Ig domains were obtained from the number of the component amino acid residues (2174 for PEVK and 95 for Ig domains) times the maximal residue spacing in an unfolded polypeptide (0.38 nm). The persistence length of the PEVK and unfolded Ig domains were set at 1.4 nm and 0.6 nm, respectively (Watanabe et al., 2002a, 2002b). (For details regarding composition of tandem Igs and PEVK of human soleus muscle see (Labeit and Kolmerer,1995).

Because the various segments that make up titin's extensible region are connected in series, they bear equal forces. Therefore, for a given force, the extension of each segment (zIg(folded), zIg(unfolded), and zPEVK) can be calculated. We may then calculate, for that force, the total extension of titin's elastic segment. By adding the total length of nonextensible sarcomeric components (1800 nm; see Trombitas et al., 1998b), the SL can be calculated as Eq. 2:

$$\mathrm{SL} = ((z\mathrm{Ig}(\mathrm{folded} + z\mathrm{Ig}(\mathrm{unfolded}) + z(\mathrm{PEVK}))\times 2 + 1800\,\mathrm{nm}) \quad (2)$$

and the predicted force-sarcomere length relation constructed.

Persistence length of PEVK containing polyproline (PP) helices

The above calculations assume that the PEVK comprises solely random coil structure. However, some of the residues may form PP helices, and, to assess the possible role of PP helix to random coil conversion in stress relaxation (see Discussion), we calculated the PEVK persistence length assuming that the PP residues are either of type II, type I, or random coil. A search for PxPP, PxxPP, and xPxxPP motifs (cf. Ma et al., 2001) suggests that 181 out of the total 2174 PEVK residues (or 8.3%) may participate in the formation of polyproline helices. The 0.31-nm translation per residue for PPII and 0.19 nm for PPI helices (Rabanal et al., 1993) allows the contour length of a 181-residue PPII and PPI helix to be calculated. We assumed that the persistence lengths of PPII and PPI helices ranged from 0.1 nm to 100 nm. The persistence length of the 1993 PEVK residues that form random coil was set at 1.4 nm (Watanabe et al., 2002b) and the contour length at 757 nm (1993 × 0.38 nm). We then calculated the force-extension curve of the 1993-residue random coil region linked with either 181-residue PPII or 181-residue PPI and compared it to the force extension curve of 2174-residue unfolded PEVK (following the methods explained above). An apparent persistence length was obtained by fitting the force versus extension curve with the WLC model, and these values were used in a serially linked WLC model with tandem-Ig and PEVK segments (above) to asses the difference in passive force-SL relation when the PEVK is completely random coil or a combination of random coil and PP helices.

Ig domain unfolding

We calculated the probability of domain unfolding under mechanical force by superimposing on the WLC force-extension curve (see above) a two-state domain unfolding/refolding kinetic model. To model domain unfolding/refolding, Monte Carlo simulations were carried out based on previously used simulation algorithms (Kellermayer et al., 2000, 2001, 1997). Briefly, for a given force (F), the number of unfolded domains were calculated according to Eq. 3:

$$dN = N\omega_0\, dt\, e^{-(E_a - FX_u)/k_BT}, \quad (3)$$

where dN is the change in the number of folded domains during the dt polling interval, N is the number of available folded domains, and X_u is the distance along the unfolding reaction coordinate between the native and main transition state. ω_0, attempt frequency, was $10^8\ s^{-1}$, and k_BT 4.14 pN nm. Unfolding events decremented the number of remaining folded domains and the length of the folded segment and increased the length of the unfolded segment, and the ensuing force was calculated according to the serially linked WLC model (see above). The activation energies (E_a) for unfolding, and X_u were user-adjustable. In all simulations we used X_u 0.28 nm and calculated activation energies from published unfolding rate constants at zero force (α_0). Our simulation also took into account refolding and assumed for refolding E_a 82 pN nm (or zero force refolding rate, 2.5 s^{-1}) and X_r 8 nm (for justification and further details, see Kellermayer et al., 2001). Refolding events incremented the number of folded domains, increased the length of the folded segment, and decreased the length of the unfolded segment. Calculations were carried out using a stretch-release protocol with a constant velocity of 100 nm/s (to match the velocity used during force measurements in muscle fibers (100 nm/s/half sarcomere), a stretch amplitude determined by the preset maximal allowable force, and a subsequent hold of a preset duration. Simulation results shown in Fig. 1 are mean ± SD values of 20 simulation runs. For additional details, see Kellermayer et al., 2000, 2001, 1997).

Rupture of bonds in PEVK

Monte Carlo simulations were also carried out assuming the presence of labile bonds that cross-link the PEVK (see Discussion), and we modeled bond rupture/formation and Ig unfolding/refolding under force, based on previously used simulation algorithms (Kellermayer et al., 2001). In this case the model molecule contained a PEVK segment whose apparent contour length is shortened by the presence of cross-links between sites along the segment (1400 sites corresponding to the approximate number of charged residues in PEVK (Labeit and Kolmerer, 1995)). As the chain was extended, force was generated according to the WLC equation. At each step,

for the given force, the number of bonds ruptured was calculated according to Eq. 4:

$$dN_{(b)} = N_b \omega_0 \, dt \, e^{-(E_{a(b)} - F\Delta X_b)/k_B T}, \quad (4)$$

where dN_b is the number of bonds broken during the dt polling interval, and N_b is the number of available bonds. Details for Ig unfolding/refolding are given above. For the bonds, the transition length (ΔX_b) and the enclosed loop perimeter (see Discussion) were randomly generated between 0.3 and 0.8 nm and between 1 and 3 nm (up to two persistence-length distances), respectively. Bond rupture events incremented the chain length with the randomly selected loop perimeter. Bond re-formation was allowed to proceed only at forces below 2 pN according to the number of available counterbinding sites (for details, see Kellermayer et al., 2001). Each bond formation event decremented the chain length with a randomly generated loop perimeter. The ensuing force was then calculated according to the serially linked WLC model (see above). The simulation results of Fig. 10 assumed a bond rupture energy $E_{a(b)}$ of 32.5 pN nm and for Ig unfolding α_0 of 5×10^{-6} s^{-1} (note that this is 100-fold lower than the 5×10^{-4} s^{-1} used in Fig. 3 *A*). The other parameters were as indicated in the Ig Domain Unfolding section above. As the chain was extended, force was generated according to a WLC equation that represents serially linked folded and unfolded subsegments, and we calculated the number of PEVK bonds ruptured, the number of unfolded Ig domains, and the WLC force. All simulations were carried out by using Object Pascal (Metrowerks CodeWarrior v.10) on an Apple PowerMacintosh G3 computer. For additional details, see Kellermayer et al., 2001).

RESULTS

Mechanical experiments were performed in which fibers were stretched with a constant velocity to a predetermined sarcomere length, held for 1 h, followed by a release back to the slack length (Fig. 1 *A*). Because IFs also contribute to passive stress, especially in long sarcomeres, experiments were conducted on fibers that had been extracted with KCl/KI. We assume that the stress after extraction was derived from IFs and stress before extraction from IFs and titin (for details, see Materials and Methods). By subtracting the passive tension after extraction (Fig. 1 *C*) from that before extraction, titin-based tension is obtained (Fig. 1 *B*), and by converting this tension to the single molecule level (see Materials and Methods) we determined the force per titin molecule as a function of time and sarcomere length. The results in Fig. 2 show that although titin-based stress relaxation is most prominent immediately after stretch, force continues to decay during the 1-h hold period, albeit very slowly at the end, with an ~50% reduction in force between 1 and 60 min (see inset of Fig. 2).

To assess whether unfolding of Ig domains explains stress relaxation, we performed a Monte Carlo simulation of unfolding/refolding superimposed on the force-extension curve of serially linked WLCs, representing tandem-Ig segments and the PEVK sequence of human soleus titin (see Materials and Methods). Using unfolding parameters of I91 (formerly I27), measured by AFM (α_0: 5×10^{-4} s^{-1}; X_u: 0.28 nm (Carrion-Vazquez et al., 1999)), and simulating an ~10-s hold, reveals unfolding of several Ig domains and a degree of stress relaxation that simulates well the measured stress relaxation (Fig. 3 *A*). Similar conclusions were drawn by Minajeva et al. (2001), who used a Monte Carlo simulation with the same unfolding parameters as used here, and who were able to effectively simulate stress relaxation displayed by myofibrils during a 4-s hold. Consistent with Minajeva et al. (2001), varying α_0 results in simulated stress relaxation that fits the data best when α_0 is 5×10^{-4} s^{-1}. The broken lines in Fig. 1 *A* indicate, for example, that when α_0 is 1×10^{-7} s^{-1}, unfolding is absent during the 10-s hold (see Discussion for why this low α_0 was selected for display).

Expanding the hold period to an hour and using the same unfolding kinetics that successfully explain short-term stress

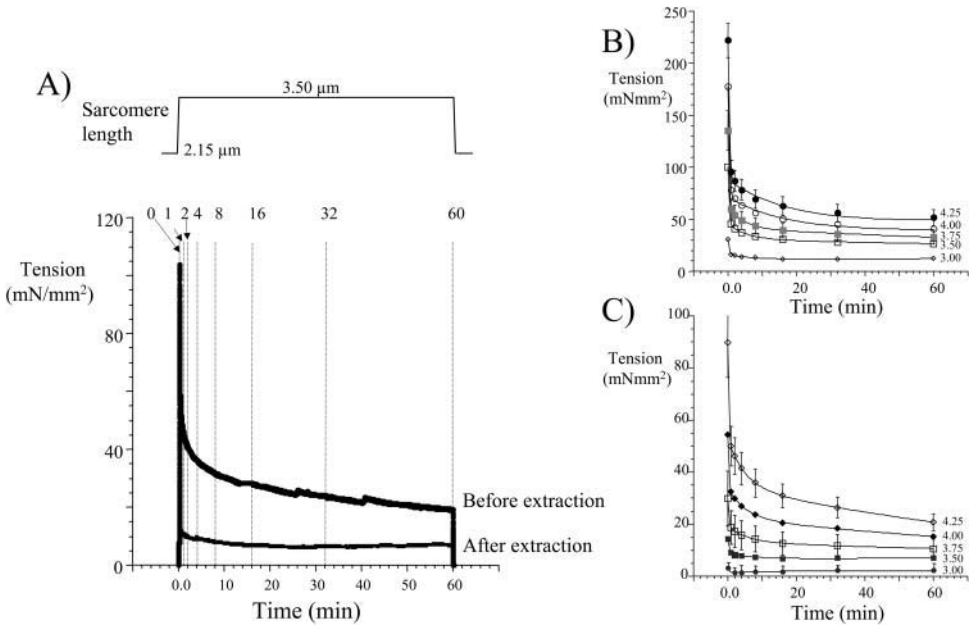

FIGURE 1 Measured stress relaxation in passive soleus fibers. (*A*) Protocol: fiber was stretched and then held for 1 h followed by a release. *Top*, sarcomere length; *bottom*, passive tension. The protocol was repeated after KCl/KI extraction (see Materials and Methods). The KCl/KI-sensitive tensions of fibers that had been stretched to different SLs are shown in *B* and the KCl/KI-insensitive tensions in *C*. (Mean ± SD of six fibers. Each fiber contributed data to both *B* and *C*. Data in *B* and *C* were obtained by stretching the fiber from the same initial SL of ~2.1 μm. For simplicity's sake only selected time points (indicated in *A*, *bottom*) are shown in *B* and *C*; see text for additional details.)

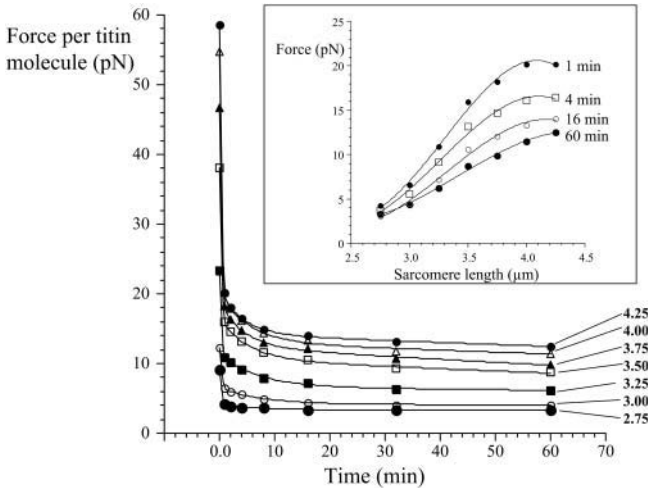

FIGURE 2 Measured titin-based force versus time at a range of SLs. Titin-based tension was assumed to be equal to the KCl/KI-sensitive tension (same data as in Fig. 1 *B*), and measured tensions (in mN/mm^2) were converted to force per titin molecule (see Materials and Methods). (*Inset*) Data converted to force-SL relations 1, 4, 16, and 60 min after completion of stretch. (Mean results from six fibers are shown. Numbers at bottom right correspond to sarcomere lengths in μm.)

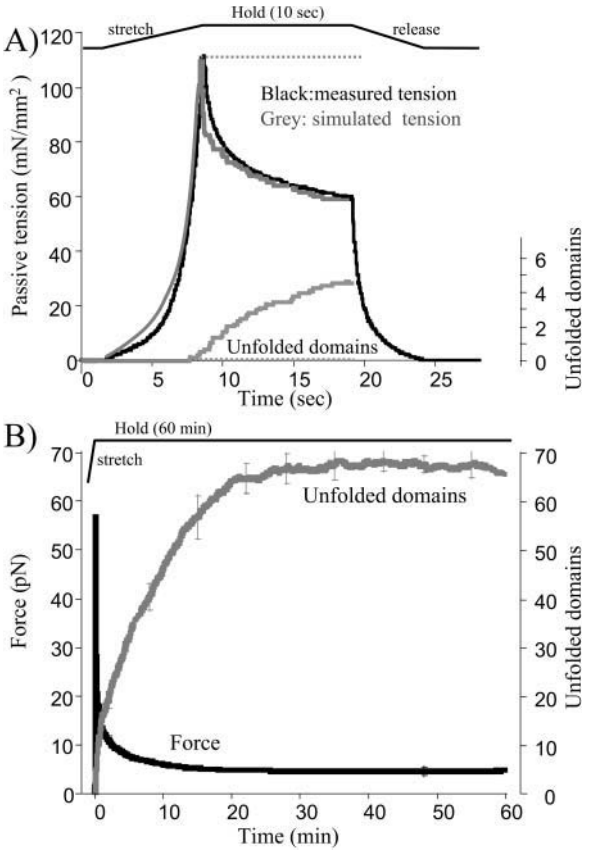

FIGURE 3 (*A*) Measured passive tension (*black*), simulated passive tension (*gray*), and simulated Ig domain unfolding (*gray*, *bottom*) during stretch-hold protocol. During 10-s hold, simulation reveals unfolding of four Ig domains and a predicted decay of passive tension that approximates well the measured tension (measured after stretch from sarcomere length 2.1 μm to 4.0 μm). Simulation assumes α_0 5 $\times$ 10^{-4} s^{-1}. The broken lines indicate predicted force (*top*) and predicted unfolding (*bottom*) for α_0 of 1 $\times$ 10^{-7} s^{-1}. (*B*) Simulated passive force of single titin molecule in sarcomere during 1-h hold period. The molecule was stretched to a peak force of 56 pN (chosen because this is the measured peak force when stretched to SL 4.0 μm, see Fig. 2). During the hold, unfolding of Ig domains is predicted to continue until a maximum of 70 domains are unfolded. Passive force is predicted to decay until a steady value of ~5 pN is reached. (Simulations assume for unfolding X_u 0.28 nm; α_0 5 $\times$ 10^{-4} s^{-1}; polling interval 0.01 s; stretch velocity 100 nm/s. For refolding characteristics and additional details, see Materials and Methods. *Upper black traces* in each figure represent the sarcomere length changes during the protocol.)

relaxation (Fig. 3 *A*) reveals that unfolding and stress relaxation proceed until the majority of the domains are unfolded (70 in the example shown in Fig. 3 *B*) and force is very low (~5 pN in Fig. 3 *B*). (Not all domains will unfold because when stress relaxation reaches low forces, refolding takes place (the refolding process is also included in our simulation; see Materials and Methods), and eventually an equilibrium is reached in which the number of unfolding and refolding events are in balance). Thus, simulation results predict a large number of unfolded Ig domains during extensive time periods of stress relaxation, the consequence of which on tandem-Ig segment lengths can be tested by using immunoelectron microscopic methods.

Immunoelectron microscopy

Large-scale Ig unfolding is expected to result in lengthening of the tandem-Ig segments (at the expense of shortening of the PEVK segment). To test whether this indeed occurs, we used IEM and measured the end-to-end lengths of the tandem-Ig segments in fibers that had been stretched, held, fixed, and immunolabeled (for details, see Materials and Methods). The antibodies that were used in this work are shown in Fig. 4 *A*, and typical labeling results in Fig. 4 *A* (*bottom*) and Fig. 4, *B–D*. Some fibers were fixed immediately after stretch (stretch was performed as in mechanical experiments, see above, and fixative was added within ~1 s after stretch was completed), others after a long hold phase (up to 64 h). Based on our simulations (Fig. 3 *B*) we anticipated much-elongated tandem-Ig segments in fibers held for several tens of minutes, but because preliminary findings (not shown) failed to reveal the expected results, we decided to extend the hold period to 64 h (the longest possible hold period that was practical). Results shown in Fig. 5 *A* reveal only minimal differences between fibers fixed immediately after stretch and those held for 64 h. At intermediate sarcomere lengths, the distal tandem-Ig segment was ~20 nm longer after the long hold period (Fig. 5 *B*), but no other clear differences were found for this or any of the other segment types (Fig. 5, *B–D*). The expected behavior of tandem-Ig and PEVK segments assuming unfolding of 70 domains (see Materials and Methods) was superimposed on the measured segment lengths (see Fig. 6).

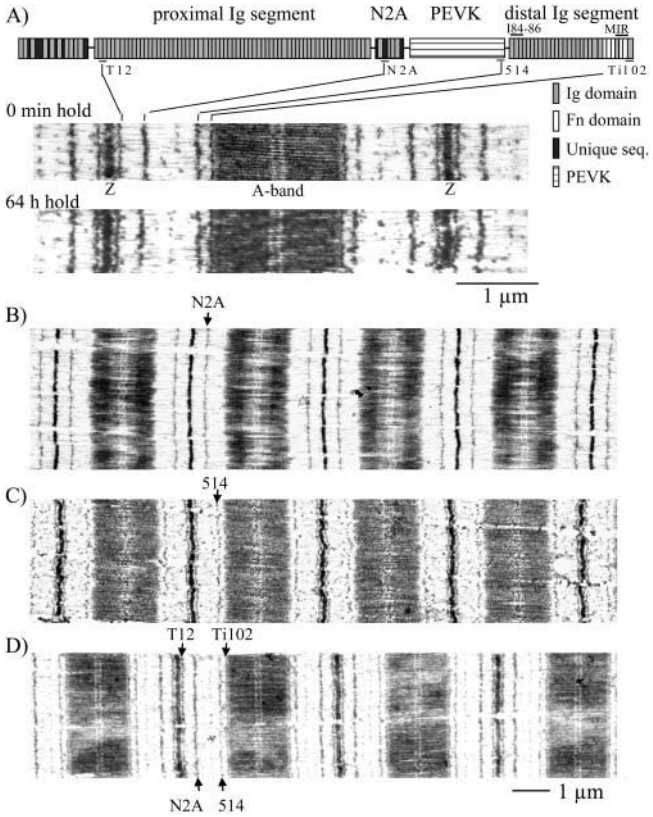

FIGURE 4 Immunoelectron microscopy of titin. (*A*) *Top*, sequence of I-band region of soleus titin (Labeit and Kolmerer, 1995). Indicated are the binding sites of T12, N2A, 514, I84-86, MIR, and Ti102 antibodies. *Bottom*, sarcomeres simultaneously labeled with four antibodies. Fibers were stretched and then held for 0 min (*top*) or 64 h (*bottom*) followed by fixing and labeling. (*B–D*) Additional examples of electron micrographs of fibers labeled with anti-titin antibodies used in this work. (Sarcomere lengths: *A*, 4.1 μm; *B*, 3.6 μm; *C*, 3.5 μm; and *D*, 4.2 μm.)

This comparison reveals that our results are inconsistent with the presence of large-scale unfolding (although they do not exclude unfolding of a few domains, see Discussion). To ascertain whether unfolding of domains may have been missed in the ''zero min hold dataset'' due to slowness of the speed of chemical fixation (see Materials and Methods), we measured passive stiffness using small amplitude (~0.1%) stretch-release protocols and used stiffness increase as a measurement of degree of fixation. Adding fixative resulted in a rapid increase of passive stiffness with a $T_{1/2}$ of 9.8 ± 3.3 s ($n = 4$). Thus, although a small degree of Ig unfolding may take place between applying the fixative and the ensuing chemical fixation, it is unlikely that large-scale unfolding had taken place in the ''zero min hold dataset'', and that this explains why segment lengths after long-term hold overlap with those after a hold of zero min. Instead, our data suggest that large-scale unfolding is absent.

To determine whether there are some conditions in which Ig domains can be forced to unfold, we performed a set of experiments in which the stretch amplitude was extended beyond the sarcomere length range with reversible passive mechanics. Irreversible behavior at extreme sarcomere lengths is likely to result from structural damage to the thick filaments and release of titin from the A-band region (Wang et al., 1993) and may have other sources as well. Overstretch resulted in absence of labeling with the MIR and Ti-102 antibodies, which normally label at the edge of the A-band (absence of labeling precluded study of the distal tandem-Ig segment). Results shown in Fig. 7 reveal that when sarcomere length exceeded ~4.5 μm, the proximal tandem-Ig segment greatly extended (PEVK extension was absent; see inset of Fig. 7, *bottom*), suggesting that at extreme sarcomere lengths Ig unfolding can indeed be induced.

Effect of thin filament extraction on Ig domain unfolding

An important distinction between Ig domain unfolding assessed by AFM experiments and fiber experiments is that in the sarcomere, thin filaments are present in the vicinity of titin. To determine whether the presence of thin filaments slows Ig unfolding (for example, due to weak binding of Ig domains to the thin filament), experiments were performed on fibers that had been treated with gelsolin. Fig. 8 *A* shows that this largely removed thin-filament proteins (the small amount of remaining actin is likely to reflect extraction-resistant actin in the Z-line region of the sarcomere (Granzier and Wang, 1993c)) and nebulin, without influencing thick-filament–based proteins and titin. As shown in Fig. 8 *B*, passive tension after extraction was slightly elevated (such increase has been reported earlier and was ascribed to the recruitment of near Z-line titin to the extensible titin pool (Granzier et al., 1997)). The time course of stress relaxation was not affected by thin-filament extraction. IEM experiments were focused on the proximal tandem-Ig segment, and results are shown in Fig. 9. Although results were relatively scattered, they do allow for the conclusion that thin filament extraction with gelsolin had no major effect on extension of the proximal tandem-Ig segment. All together, our observations indicate that the unfolding of Ig domains is not facilitated by removal of the thin filament.

DISCUSSION

Immunoglobulin type I and fibronectin type III domains were the first sequence elements discovered in titin (Labeit et al., 1990). Early models of titin elasticity (Erickson, 1994) were based on the reversible unfolding and refolding of these domains. The subsequent discovery of the PEVK segment in titin (Labeit and Kolmerer, 1995) suggested that the molecule might extend without the unfolding of globular domains. Indeed, IEM revealed that in skeletal muscle, the PEVK provides the majority of extensibility in intermediate to long sarcomeres (Linke et al., 1998a; Trombitas et al., 1998a,b). Tandem-Ig segments were shown to extend mainly

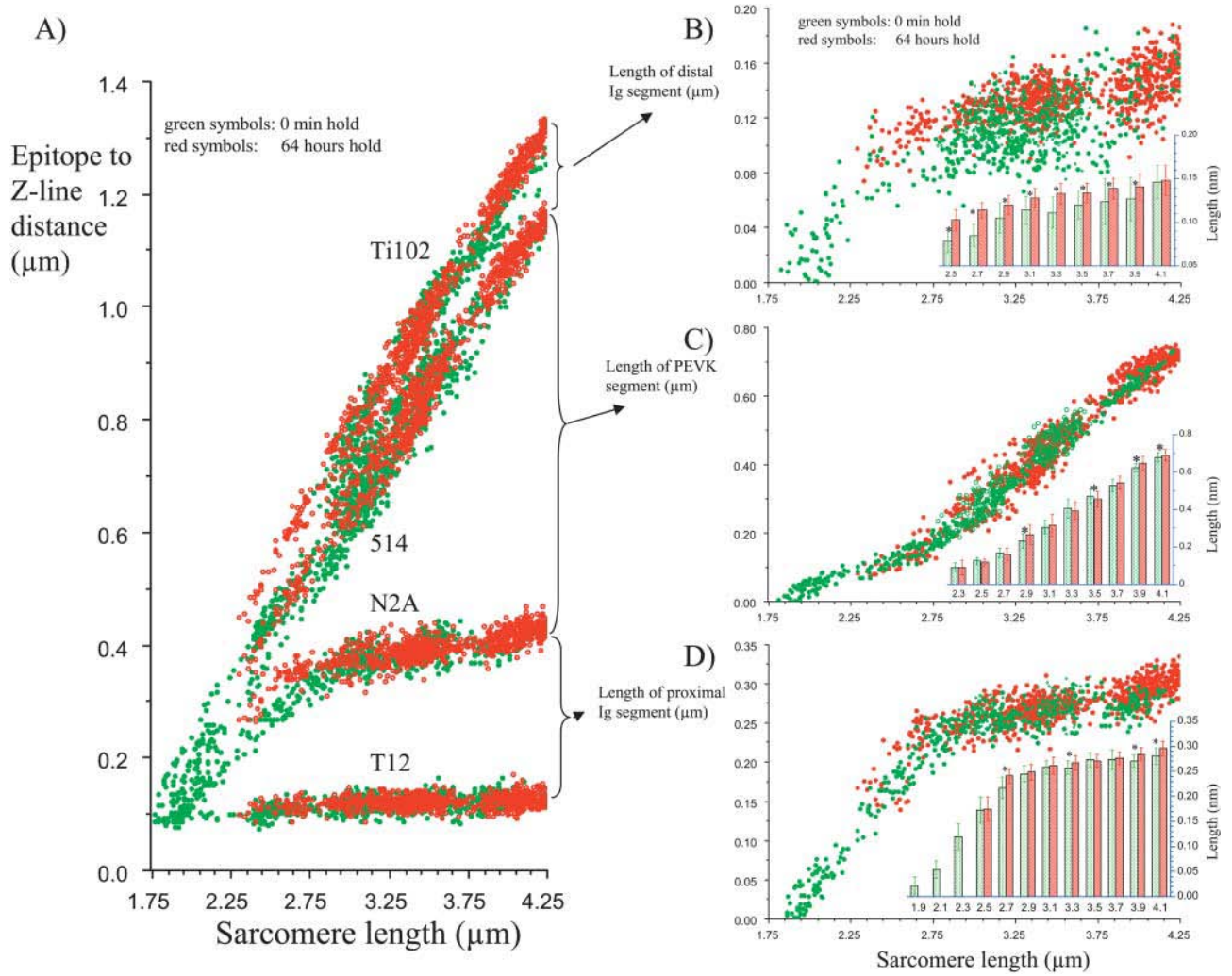

FIGURE 5 (*A*) Mid-epitope to mid-Z-line distance of T12, N2A, 514, and Ti102 epitopes in fibers stretched and held for 0 min (*green symbols*) and 64 h (*red symbols*). Length of proximal and distal tandem-Ig segment: distance from T12 to N2A and from 514 to Ti102, respectively. Length of PEVK: distance from N2A to 514 eptiopes. (*B–D*) Lengths of tandem-Ig and PEVK segments versus sarcomere length of fibers stretched and held for 0 min and 64 h. Insets show mean and SD of results binned in 0.1 μm SL bins. Asterisks denote statistically significant differences ($P < 0.05$).

before PEVK extension and then attain a nearly constant length that can be accommodated by folded domains. Thus, the notion emerged that the Ig domains form stable structures that function as ''spacers'' that set the minimal sarcomere length at which PEVK segment extension dominates (Linke and Granzier, 1998). This view was recently challenged, however, by Minajeva et al. (2001) who sought to explain stress relaxation in myofibrils and utilized Ig unfolding characteristics that had been measured at the single molecule level by AFM. When tandem-Ig segments are forcibly elongated by AFM (Carrion-Vazquez et al., 2000; Rief et al., 1997), unfolding of Ig domains can be observed (typically at forces >200 pN), and by measuring the stretch-rate dependence of the unfolding force, the unfolding rate constant at zero force (α_0) and the distance along the unfolding reaction coordinate between the native and main transition state (X_u) can be deduced. A Monte Carlo simulation of Ig domain behavior in stretch-hold protocols revealed that unfolding of several domains effectively simulated stress relaxation during a 4-s hold period (Minajeva et al., 2001). Our short-term hold simulation experiments (Fig. 3 *A*) confirm this result. However, allowing the simulation to proceed further in time results in continuing, progressive unfolding until the majority of the domains are unfolded (Fig. 3 *B*). Thus, unfolding characteristics of Ig domains that well explain stress relaxation during short-term hold protocols give rise to large-scale unfolding in long-term hold protocols.

Measurement of tandem-Ig segment length during long-term stress relaxation

Because unfolding of a single domain results in contour length gain of ~30 nm, large-scale unfolding during stress relaxation is predicted to greatly increase the length of the

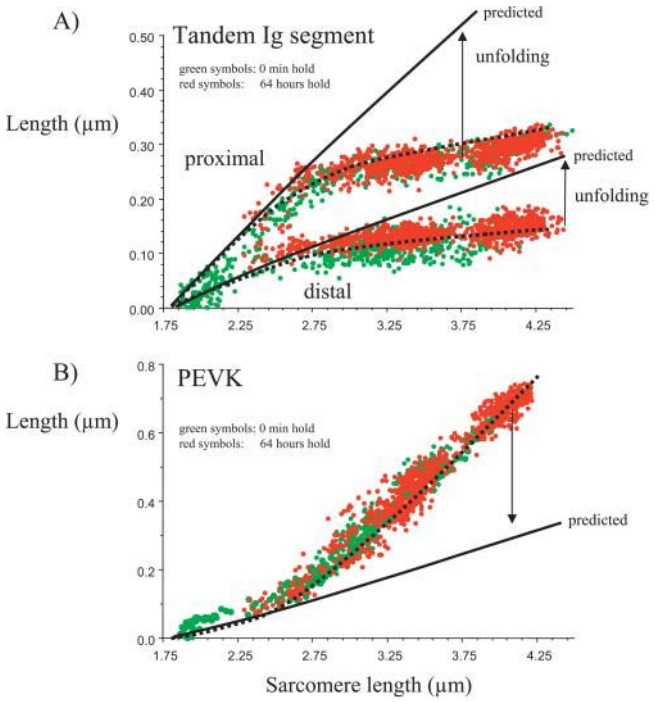

FIGURE 6 Measured and predicted lengths of tandem-Ig (*A*) and PEVK (*B*) segments. Measured: green symbols, fibers stretched and then held for 0 min; red symbols held for 64 h. Broken lines are predicted extensions assuming that Ig unfolding is absent and solid lines assuming that a total of 70 domains are unfolded. We assumed that of the 70 unfolded domains, 50 are in the proximal and 20 in the distal segment (the difference reflects the proportion of the total number of domains contained in the segments). (Prediction based on serially linked wormlike chains model in which folded and unfolded tandem-Ig subsegments as well as the PEVK are represented. For details, see Materials and Methods.)

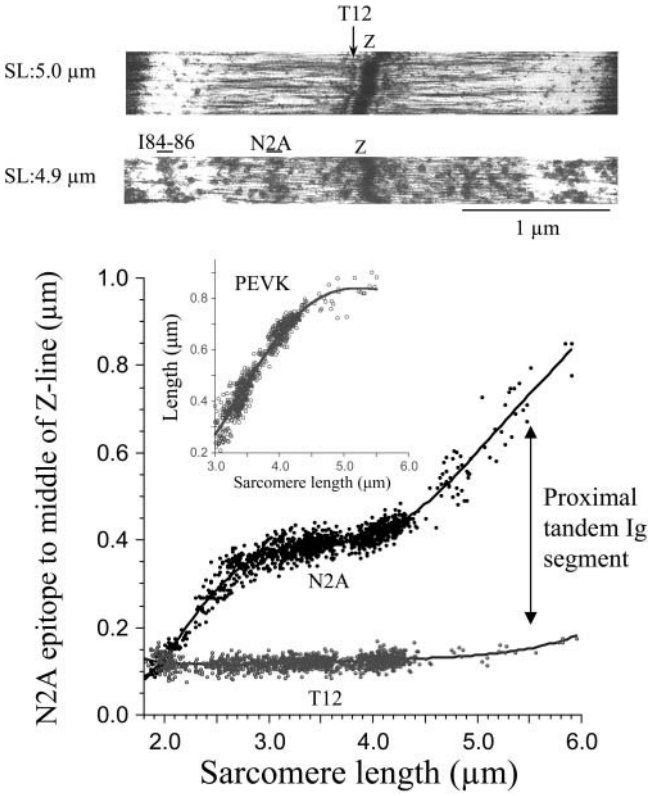

FIGURE 7 Behavior of N2A and T12 epitopes in extremely long sarcomeres. (*Top*) Examples of labeled sarcomeres (only I-band regions are shown). (*Bottom*) Scattergram of results. At SLs > ~4.5 μm the proximal tandem-Ig segment greatly extends. Inset in bottom graph shows length of PEVK (distance between N2A and I84-86 epitopes). Note that extension of proximal tandem-Ig segment at long SLs coincides with a near constant PEVK segment length.

tandem-Ig segments (see arrows in Fig. 6 *A*), and our aim was to test this prediction by studying fibers that had been held at a constant length for various durations. Results of our IEM study, however, failed to reveal the predicted length increase of tandem-Ig segments, even when the stress-relaxation period was extended to 64 h. To determine whether this failure is due to technical inadequacies, we performed experiments on overstretched fibers with sarcomere lengths as long as 6.0 μm. Although this results in irreversible structural damage to the sarcomeres (Wang et al., 1993), we were able to label the ends of the proximal tandem-Ig segment (Fig. 7, *top*) and show that this segment was greatly elongated when long-term stress relaxation was induced at sarcomere lengths >4.5 μm (Fig. 7, *bottom*). Thus, the constant segment length observed during stress relaxation in sarcomeres shorter than ~4.25 μm (Fig. 6 *A*), which includes the physiological length range, is unlikely due to our inability to detect length changes, but instead to absence of large-scale unfolding.

Our findings indicate that under physiological force conditions and in the context of the structural arrangement of the sarcomere, Ig domains are more stable than expected from single molecule measurements made in vitro with AFM. Monte Carlo simulation indicates that an unfolding rate constant (α_0) of $\sim 1 \times 10^{-7}$ s^{-1} is required to explain the near-constant tandem-Ig segment lengths at the measured passive force levels. It is unlikely that thin filaments stabilize Ig domains in the sarcomere, because their removal from the sarcomere has no effect on the length of the tandem-Ig segment (Fig. 9). Instead, we consider it likely that the AFM measurements, all of which are made using loading conditions that far exceed physiological levels, do not extrapolate to the conditions that exist in the sarcomere and that they underestimate Ig domain stability under physiological conditions. This notion is consistent with the recent work of Williams et al. (2003) who performed AFM-based mechanical unfolding studies on wild-type and various mutants of a domain from the distal tandem-Ig segment (I91, formerly I27). Their study provides evidence that α_0 varies with the loading range used to deduce this parameter, supporting that domains may be able to withstand higher force under physiological conditions than predicted from AFM experiments conducted at high load. Thus, to understand the contribution of titin's subsegments to muscle mechanics, titin must be studied under physiological conditions. When the role of

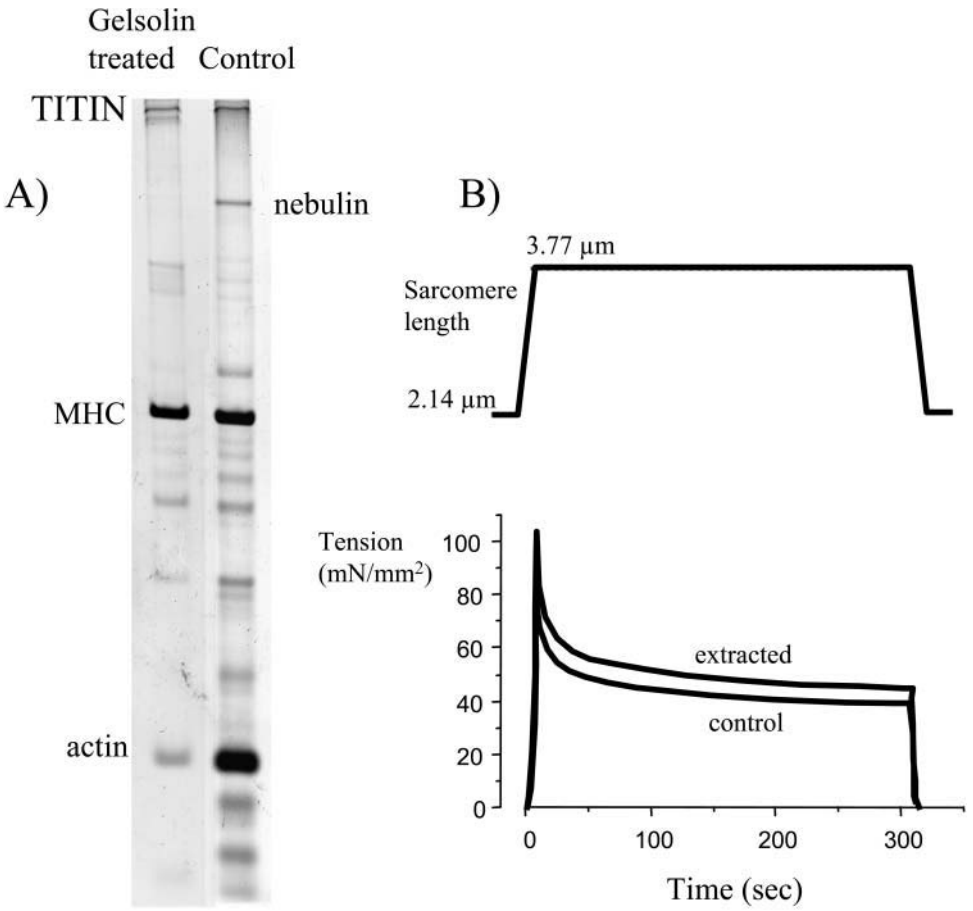

FIGURE 8 Effect of thin filament removal with gelsolin on protein composition (*A*) and passive tension (*B*). The gel of single fibers in *A* reveals that gelsolin largely removed actin and nebulin without major effect on titin and myosin heavy chain (MHC); mechanical measurements in *B* revealed that thin filament extraction slightly elevated passive tension.

tandem-Ig segments in stress relaxation is examined in muscle fibers, appreciable domain unfolding is absent.

Molecular basis of stress relaxation

Because of the serial linkage of the various segments that make up titin's extensible region (proximal and distal tandem-Ig segments and PEVK), all segments will experience the same external force, i.e., a force that during long-term hold protocols progressively decreases with time (as in Fig. 3). This decreasing force will result in a reduction in the length of those segments with mechanical characteristics that remain unaltered during stress relaxation. Our finding that neither tandem-Ig nor PEVK segments shorten during long-term stress relaxation (Figs. 5 and 6) implies that mechanical alterations in both segment types must take place. Although large-scale Ig domain unfolding is made unlikely by our measurements, as discussed above, the measurement of tandem-Ig segment length (Fig. 6) in conjunction with passive stress relaxation (Fig. 3) suggests that structural transitions must occur in the segment that modify its overall mechanical characteristics. A possible candidate is lengthening of domains without complete unfolding. The presence of unfolding intermediates has been deduced from a ''hump'' on the force-extension curve seen when domains are stretched (Marszalek et al., 1999), and if these intermediate states were to become progressively populated during long-term hold protocols, stress relaxation could ensue. However these unfolding intermediates seem to occur only in domains from the distal tandem-Ig segment (Li et al., 2002), and they cannot explain the observed behavior of the proximal tandem-Ig segment. An alternative explanation is that a few Ig domains contained within the segment completely unfold. Unfolding of each domain will increase the contour length of the tandem-Ig segment by ~30 nm and decrease its overall persistence length (from ~15 nm for the fully folded chain to ~0.6 nm for the fully unfolded chain). By modeling the tandem-Ig segment as a serially linked chain of folded and unfolded subsegments, one may calculate (see Materials and Methods for details) that unfolding of a single domain during the first 1 min of stress relaxation and 2 domains during the subsequent 59 min of stress relaxation allows the proximal tandem-Ig segment to remain at near constant length while experiencing the forces shown in Fig. 2. Calculations reveal that a similar degree of unfolding in the distal tandem-Ig segment can explain its measured length (Fig. 5 *B*) and force as a function of time (Fig. 2). Thus a very limited degree of Ig unfolding may occur during the long-term hold.

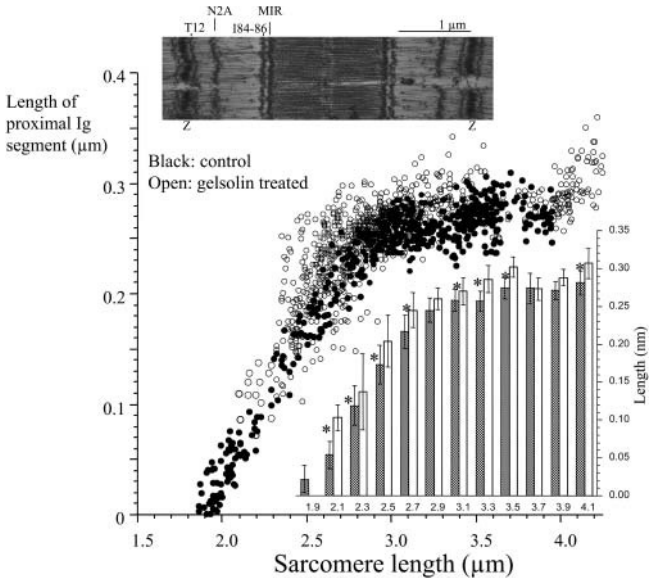

FIGURE 9 Effect of thin filament removal on length of proximal tandem Ig (T12-N2A distance). Top shows example of thin-filament extracted and titin-labeled sarcomere. Bottom right inset shows mean and SD of results binned in 0.1 μm SL bins (*gray bars*, control; *open bars*, gelsolin treated). Asterisks denote statistically significant differences ($P < 0.05$).

Whether unfolding events occur randomly within the Ig domain population or whether certain domains are specialized for unfolding remains to be established. Unfolding increases the contour length (C) of the tandem-Ig segment, and the ensuing reduction in fractional extension (z/C) allows the segment to remain at constant length (z) while experiencing a reduction in force.

As for the PEVK segment, its length also remains virtually constant during long-term stress relaxation (Fig. 5 *C*), indicating that the PEVK also must undergo structural changes. Although the PEVK was originally assumed to consist of largely random coil, evidence has been obtained recently (Ma et al., 2001) that some of the PEVK residues may form polyproline (PP) helix structure. In the soleus PEVK, 181 out of the total 2174 PEVK residues (or 8.3%) may be part of polyproline helices (see Materials and Methods). If during stress relaxation these PP helices were to gradually unfold and convert to random coil, the ensuing contour length gain could give rise to a reduction in force. Estimating how much this may contribute to stress relaxation is hampered by the unknown persistence length of PP helices. Calculations that assume a wide range of values (see Materials and Methods) reveal that at most they can account for ~40% of the observed stress relaxation, and that this requires assuming an unrealistically low PP helix persistence length (0.1 nm). Thus unfolding of PP helices can, at most, account for part of the stress relaxation observed in PEVK.

Another possible explanation for PEVK-based stress relaxation is a mechanism that we recently proposed for explaining molecular fatigue in single titin molecules stretched by laser-tweezers, a mechanism in which labile bonds that cross-link various sites along the PEVK rupture upon stretch (Kellermayer et al., 2001). Although the exact nature of these intrachain bonds remains to be established, considering that the PEVK segment carries a preponderance of charged residues (Labeit and Kolmerer, 1995), they may be electrostatic. The positively charged PPAK and negatively charged polyglutamic acid domains might be involved in these interactions (Greaser, 2001). Evidence for such bonds has recently been obtained from circular dichroism measurements on PPAK and polyE peptide mixtures (M. Greaser, personal communication). The presence of cross-links between sites along the PEVK segment shortens the effective contour length of the segment, and external force may rupture these bonds and increase the apparent contour length according to the length of the molecule segment (perimeter) each bond

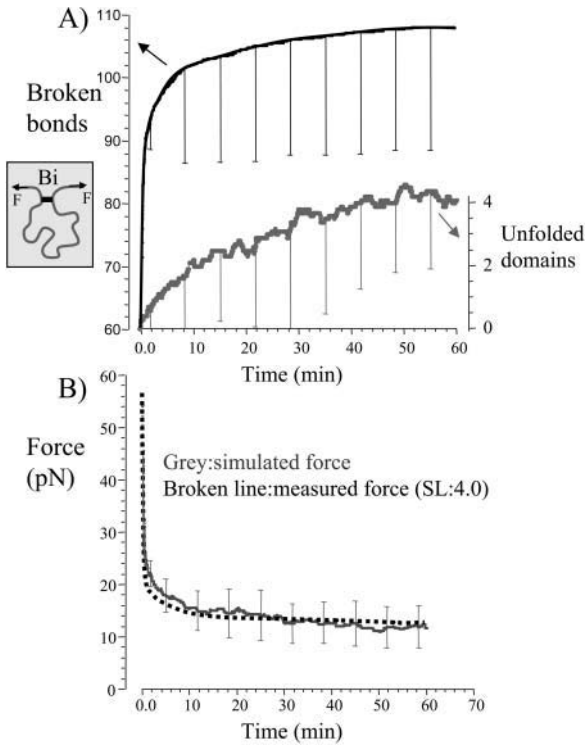

FIGURE 10 Model in which unfolding of Ig domains and breakage of random bonds in titin's PEVK region give rise to stress relaxation. Results of Monte Carlo simulation (for details see Materials and Methods) in which molecule was stretched to a maximal force of 56 pN and the number of broken bonds and unfolded domains was calculated during a 1-h hold period. Top left shows a schematic of a bond, Bi. The bond shields part of the chain from external force and removes it from contributing to the contour length. Upon bond breakage, the contour length increases, fractional extension is reduced, and force falls. (*A*) After stretching to high force and then holding the molecule at constant length, the predicted number of broken bonds increases initially fast and then more gradually. The number of unfolded Ig domains (*right scale*) gradually increases to ~4 domains at the end of the 1-h hold phase. (*B*) Simulated and measured force (SL 4.0 μm; same data as in Fig. 3). Note that simulated forces closely follow measured forces. (Shown are the mean ± SD values of 20 simulation runs. For simulation parameters and other details, see Materials and Methods.)

encloses (schematic in Fig. 10 *A*, left). If such rupture occurs at a constant end-to-end length of the PEVK, fractional extension will be reduced, and so will be force.

Monte Carlo simulations were carried out to model bond rupture/formation in the PEVK and domain unfolding/refolding in tandem-Ig segments, based on previously published simulation algorithms (Kellermayer et al., 2001). The Monte Carlo simulation of stretching the molecule to high force and then holding it for an extended period (see Materials and Methods for details) results initially in breakage of a large number of PEVK bonds that rapidly decreases force, and subsequently in a slow increase in the number of broken bonds, accompanied by a more gradual reduction of force and the appearance of gradual unfolding of a few Ig domains (Fig. 10). The simulation results are overall consistent with the measurements (Fig. 10 *B*) and lend support for a stress-relaxation mechanism based on rupture of intrachain cross-links. This hypothesized mechanism requires experimental testing, as do other possible mechanisms, including cross-links between adjacent molecules.

CONCLUSION

Immunolabeling studies on relaxed human soleus muscle fibers show that under physiological loading conditions Ig domains are more stable than predicted by AFM experiments and that Ig domain unfolding cannot solely explain passive stress relaxation. Functions of Ig domains include a ''spacer function'' that sets the minimal sarcomere length at which PEVK segment extension dominates and a ligand binding function (Granzier and Labeit, 2002); our work suggests that these functions require that Ig domains maintain their folded state.

We thank Dr. J.-P. Jin for providing us with the Ti-102 antibody. M.S.Z.K. is a Howard Hughes Medical Institute Investigator International research scholar.

This work was supported by the National Institutes of Health (HL61497 and HL62881 to H.G.; HL62466 to M.G.), Deutsche Forschungsgemeinschaft (La668/6-2 and 7-1 to S.L.), and Hungarian Science Foundation (OTKA T037935 to M.S.Z.K.).

REFERENCES

Bang, M. L., T. Centner, F. Fornoff, A. J. Geach, M. Gotthardt, M. McNabb, C. C. Witt, D. Labeit, C. C. Gregorio, H. Granzier, and S. Labeit. 2001. The complete gene sequence of titin, expression of an unusual approximately 700-kDa titin isoform, and its interaction with obscurin identify a novel Z-line to I-band linking system. *Circ. Res.* 89:1065–1072.

Bustamante, C., J. F. Marko, E. D. Siggia, and S. Smith. 1994. Entropic elasticity of lambda-phage DNA. *Science.* 265:1599–1600.

Carrion-Vazquez, M., A. F. Oberhauser, T. E. Fisher, P. E. Marszalek, H. Li, and J. M. Fernandez. 2000. Mechanical design of proteins studied by single-molecule force spectroscopy and protein engineering. *Prog. Biophys. Mol. Biol.* 74:63–91.

Carrion-Vazquez, M., A. F. Oberhauser, S. B. Fowler, P. E. Marszalek, S. E. Broedel, J. Clarke, and J. M. Fernandez. 1999. Mechanical and chemical unfolding of a single protein: a comparison. *Proc. Natl. Acad. Sci. USA.* 96:3694–3699.

Cazorla, O., A. Freiburg, M. Helmes, T. Centner, M. McNabb, Y. Wu, K. Trombitas, S. Labeit, and H. Granzier. 2000. Differential expression of cardiac titin isoforms and modulation of cellular stiffness. *Circ. Res.* 86:59–67.

Cazorla, O., G. Vassort, D. Garnier, and J. Y. Le Guennec. 1999. Length modulation of active force in rat cardiac myocytes: is titin the sensor? *J. Mol. Cell. Cardiol.* 31:1215–1227.

Cazorla, O., Y. Wu, T. C. Irving, and H. Granzier. 2001. Titin-based modulation of calcium sensitivity of active tension in mouse skinned cardiac myocytes. *Circ. Res.* 88:1028–1035.

Erickson, H. P. 1994. Reversible unfolding of fibronectin type III and immunoglobulin domains provides the structural basis for stretch and elasticity of titin and fibronectin. *Proc. Natl. Acad. Sci. USA.* 91:10114–10118.

Fukuda, N., D. Sasaki, S. Ishiwata, and S. Kurihara. 2001. Length dependence of tension generation in rat skinned cardiac muscle: role of titin in the Frank-Starling mechanism of the heart. *Circulation.* 104:1639–1645.

Furst, D. O., M. Osborn, R. Nave, and K. Weber. 1988. The organization of titin filaments in the half-sarcomere revealed by monoclonal antibodies in immunoelectron microscopy: a map of ten nonrepetitive epitopes starting at the Z line extends close to the M line. *J. Cell Biol.* 106:1563–1572.

Granzier, H. L., H. A. Akster, and H. E. Ter Keurs. 1991. Effect of thin filament length on the force-sarcomere length relation of skeletal muscle. *Am. J. Physiol.* 260:C1060–C1070.

Granzier, H., M. Helmes, and K. Trombitas. 1996. Nonuniform elasticity of titin in cardiac myocytes: a study using immunoelectron microscopy and cellular mechanics. *Biophys. J.* 70:430–442.

Granzier, H. L., and T. C. Irving. 1995. Passive tension in cardiac muscle: contribution of collagen, titin, microtubules, and intermediate filaments. *Biophys. J.* 68:1027–1044.

Granzier, H., M. Kellermayer, M. Helmes, and K. Trombitas. 1997. Titin elasticity and mechanism of passive force development in rat cardiac myocytes probed by thin-filament extraction. *Biophys. J.* 73:2043–2053.

Granzier, H., and S. Labeit. 2002. Cardiac titin: an adjustable multifunctional spring. *J. Physiol.* 541:335–342.

Granzier, H. L., and K. Wang. 1993a. Gel electrophoresis of giant proteins: solubilization and silver-staining of titin and nebulin from single muscle fiber segments. *Electrophoresis.* 14:56–64.

Granzier, H. L., and K. Wang. 1993b. Interplay between passive tension and strong and weak binding cross-bridges in insect indirect flight muscle. A functional dissection by gelsolin-mediated thin filament removal. *J. Gen. Physiol.* 101:235–270.

Granzier, H. L., and K. Wang. 1993c. Passive tension and stiffness of vertebrate skeletal and insect flight muscles: the contribution of weak cross-bridges and elastic filaments. *Biophys. J.* 65:2141–2159.

Greaser, M. 2001. Identification of new repeating motifs in titin. *Proteins.* 43:145–149.

Gregorio, C. C., H. Granzier, H. Sorimachi, and S. Labeit. 1999. Muscle assembly: a titanic achievement? *Curr. Opin. Cell Biol.* 11:18–25.

Helmes, M., K. Trombitas, T. Centner, M. Kellermayer, S. Labeit, W. A. Linke, and H. Granzier. 1999. Mechanically driven contour-length adjustment in rat cardiac titin's unique N2B sequence: titin is an adjustable spring. *Circ. Res.* 84:1339–1352.

Higuchi, H., Y. Nakauchi, K. Maruyama, and S. Fujime. 1993. Characterization of beta-connectin (titin 2) from striated muscle by dynamic light scattering. *Biophys. J.* 65:1906–1915.

Horowits, R. 1999. The physiological role of titin in striated muscle. *Rev. Physiol. Biochem. Pharmacol.* 138:57–96.

Horowits, R., and R. J. Podolsky. 1987. The positional stability of thick filaments in activated skeletal muscle depends on sarcomere length: evidence for the role of titin filaments. *J. Cell Biol.* 105:2217–2223.

Improta, S., A. S. Politou, and A. Pastore. 1996. Immunoglobulin-like modules from titin I-band: extensible components of muscle elasticity. *Structure*. 4:323–337.

Jin, J. P. 1995. Cloned rat cardiac titin class I and class II motifs. Expression, purification, characterization, and interaction with F-actin. *J. Biol. Chem.* 270:6908–6916.

Kellermayer, M. S., S. Smith, C. Bustamante, and H. L. Granzier. 2000. Mechanical manipulation of single titin molecules with laser tweezers. *Adv. Exp. Med. Biol.* 481:111–128.

Kellermayer, M. S., S. B. Smith, C. Bustamante, and H. L. Granzier. 2001. Mechanical fatigue in repetitively stretched single molecules of titin. *Biophys. J.* 80:852–863.

Kellermayer, M. S., S. B. Smith, H. L. Granzier, and C. Bustamante. 1997. Folding-unfolding transitions in single titin molecules characterized with laser tweezers. *Science*. 276:1112–1116.

Labeit, S., D. P. Barlow, M. Gautel, T. Gibson, J. Holt, C. L. Hsieh, U. Francke, K. Leonard, J. Wardale, A. Whiting, and J. Trinick. 1990. A regular pattern of two types of 100-residue motif in the sequence of titin. *Nature*. 345:273–276.

Labeit, S., and B. Kolmerer. 1995. Titins: giant proteins in charge of muscle ultrastructure and elasticity. *Science*. 270:293–296.

Li, H., W. A. Linke, A. F. Oberhauser, M. Carrion-Vazquez, J. G. Kerkvliet, H. Lu, P. E. Marszalek, and J. M. Fernandez. 2002. Reverse engineering of the giant muscle protein titin. *Nature*. 418:998–1002.

Linke, W. A. 2000. Stretching molecular springs: elasticity of titin filaments in vertebrate striated muscle. *Histol. Histopathol.* 15:799–811.

Linke, W. A., and H. Granzier. 1998. A spring tale: new facts on titin elasticity. *Biophys. J.* 75:2613–2614.

Linke, W. A., M. Ivemeyer, P. Mundel, M. R. Stockmeier, and B. Kolmerer. 1998a. Nature of PEVK-titin elasticity in skeletal muscle. *Proc. Natl. Acad. Sci. USA*. 95:8052–8057.

Linke, W. A., M. Ivemeyer, N. Olivieri, B. Kolmerer, J. C. Ruegg, and S. Labeit. 1996. Towards a molecular understanding of the elasticity of titin. *J. Mol. Biol.* 261:62–71.

Linke, W. A., D. E. Rudy, T. Centner, M. Gautel, C. Witt, S. Labeit, and C. C. Gregorio. 1999. I-band titin in cardiac muscle is a three-element molecular spring and is critical for maintaining thin filament structure. *J. Cell Biol.* 146:631–644.

Linke, W. A., M. R. Stockmeier, M. Ivemeyer, H. Hosser, and P. Mundel. 1998b. Characterizing titin's I-band Ig domain region as an entropic spring. *J. Cell Sci.* 111:1567–1574.

Liversage, A. D., D. Holmes, P. J. Knight, L. Tskhovrebova, and J. Trinick. 2001. Titin and the sarcomere symmetry paradox. *J. Mol. Biol.* 305:401–409.

Ma, K., L. Kan, and K. Wang. 2001. Polyproline II helix is a key structural motif of the elastic PEVK segment of titin. *Biochemistry*. 40:3427–3438.

Marszalek, P. E., H. Lu, H. Li, M. Carrion-Vazquez, A. F. Oberhauser, K. Schulten, and J. M. Fernandez. 1999. Mechanical unfolding intermediates in titin modules. *Nature*. 402:100–103.

Minajeva, A., M. Kulke, J. M. Fernandez, and W. A. Linke. 2001. Unfolding of titin domains explains the viscoelastic behavior of skeletal myofibrils. *Biophys. J.* 80:1442–1451.

Price, M. G. 1984. Molecular analysis of intermediate filament cytoskeleton—a putative load-bearing structure. *Am. J. Physiol.* 246:H566–H572.

Rabanal, F., M. D. Ludevid, M. Pons, and E. Giralt. 1993. CD of proline-rich polypeptides: application to the study of the repetitive domain of maize glutelin-2. *Biopolymers*. 33:1019–1028.

Rief, M., M. Gautel, F. Oesterhelt, J. M. Fernandez, and H. E. Gaub. 1997. Reversible unfolding of individual titin immunoglobulin domains by AFM. *Science*. 276:1109–1112.

Sebestyen, M. G., J. A. Wolff, and M. L. Greaser. 1995. Characterization of a 5.4 kb cDNA fragment from the Z-line region of rabbit cardiac titin reveals phosphorylation sites for proline-directed kinases. *J. Cell Sci.* 108:3029–3037.

Trombitas, K., P. H. Baatsen, M. S. Kellermayer, and G. H. Pollack. 1991. Nature and origin of gap filaments in striated muscle. *J. Cell Sci.* 100:809–814.

Trombitas, K., A. Freiburg, T. Centner, S. Labeit, and H. Granzier. 1999. Molecular dissection of N2B cardiac titin's extensibility. *Biophys. J.* 77:3189–3196.

Trombitas, K., and H. Granzier. 1997. Actin removal from cardiac myocytes shows that near Z line titin attaches to actin while under tension. *Am. J. Physiol.* 273:C662–C670.

Trombitas, K., M. Greaser, G. French, and H. Granzier. 1998a. PEVK extension of human soleus muscle titin revealed by immunolabeling with the anti-titin antibody 9D10. *J. Struct. Biol.* 122:188–196.

Trombitas, K., M. Greaser, S. Labeit, J. P. Jin, M. Kellermayer, M. Helmes, and H. Granzier. 1998b. Titin extensibility in situ: entropic elasticity of permanently folded and permanently unfolded molecular segments. *J. Cell Biol.* 140:853–859.

Tskhovrebova, L., and J. Trinick. 2001. Flexibility and extensibility in the titin molecule: analysis of electron microscope data. *J. Mol. Biol.* 310:755–771.

Tskhovrebova, L., and J. Trinick. 2002. Role of titin in vertebrate striated muscle. *Philos. Trans. R. Soc. Lond. B Biol. Sci.* 357:199–206.

Tskhovrebova, L., J. Trinick, J. A. Sleep, and R. M. Simmons. 1997. Elasticity and unfolding of single molecules of the giant muscle protein titin. *Nature*. 387:308–312.

Wang, K., R. McCarter, J. Wright, J. Beverly, and R. Ramirez-Mitchell. 1993. Viscoelasticity of the sarcomere matrix of skeletal muscles. The titin-myosin composite filament is a dual-stage molecular spring. *Biophys. J.* 64:1161–1177.

Watanabe, K., C. Muhle-Goll, M. S. Kellermayer, S. Labeit, and H. Granzier. 2002a. Different molecular mechanics displayed by titin's constitutively and differentially expressed tandem Ig segments. *J. Struct. Biol.* 137:248–258.

Watanabe, K., P. Nair, D. Labeit, M. S. Kellermayer, M. Greaser, S. Labeit, and H. Granzier. 2002b. Molecular mechanics of cardiac titin's PEVK and N2B spring elements. *J. Biol. Chem.* 277:11549–11558.

Williams, P. M., S. B. Fowler, R. B. Best, J. Luis Toca-Herrera, K. A. Scott, A. Steward, and J. Clarke. 2003. Hidden complexity in the mechanical properties of titin. *Nature*. 422:446–449.

Wu, Y., O. Cazorla, D. Labeit, S. Labeit, and H. Granzier. 2000. Changes in titin and collagen underlie diastolic stiffness diversity of cardiac muscle. *J. Mol. Cell. Cardiol.* 32:2151–2162.

Yu, F. X., D. M. Zhou, and H. L. Yin. 1991. Chimeric and truncated gCap39 elucidate the requirements for actin filament severing and end capping by the gelsolin family of proteins. *J. Biol. Chem.* 266:19269–19275.